LOW-IMPEDANCE THIN-FILM AlN-ON-DIAMOND

LATERAL-EXTENSIONAL RESONATORS

By

HEDIYEH FATEMI

Bachelor of Science in Electrical Engineering

University of Tehran

Tehran, Iran

2009

Submitted to the Faculty of the
Graduate College of the
Oklahoma State University
in partial fulfillment of
the requirements for
the Degree of
MASTER OF SCIENCE
December, 2011

LOW-IMPEDANCE THIN-FILM AlN-ON-DIAMOND

LATERAL-EXTENSIONAL RESONATORS

Thesis Approved:

Dr. Reza Abdolvand
_____
Thesis Adviser

Dr. Daryoosh Vashaee
_____

Dr. John M. Acken
_____

Dr. Sheryl A. Tucker
_____
Dean of the Graduate College

.

Dedicated to my parents

TABLE OF CONTENTS

LIST OF TABLES

LIST OF FIGURES

CHAPTER 1

INTRODUCTION

There is a high demand for resonators in the communication systems as the building blocks for frequency synthesis (oscillators) and/or frequency selection (filters). IC technology has enabled implementing passive resonators along with other electronic components on the small area of a chip. However, these purely electronic resonators (LC resonators) take up a lot of room on the chip and become very lossy and inefficient at higher frequencies. Resonators that take advantage of mechanically-vibrating elements (e.g. quartz crystals and tuning forks), have been developed and used in many applications but these devices are relatively large and cannot be integrated. So, there was still the need for resonators with low insertion loss that can be designed for a large frequency range while being compatible with CMOS technology. Microelectromechanical system (MEMS) is an emerging technology that offers new different techniques to build on-chip resonators.

In this thesis, we discuss thin-film piezoelectric-on-substrate (TPoS) resonators, as one class of piezoelectric micromachined resonators. The substrate of the resonators is chosen from the materials with high energy density, low acoustic loss, and high acoustic velocity. Diamond was chosen as the substrate for the TPoS resonators presented in this work due to its high acoustic velocity that permits reaching high frequencies without sacrificing the ease of fabrication. This

work is dedicated to optimize the performance of these resonators to have low insertion loss for the target frequencies in the VHF and UHF bands. Also, a ~900MHz resonator is reported with the lowest insertion loss (2.6 dB) reported till the date.

This thesis is prepared in 6 chapters. Chapter 1 is a brief introduction to the focus of this work. Chapter 2 reviews the different classes of micromachined resonators along with the advantages and disadvantages of each class. Chapter 3 thoroughly explains the concept of the TPoS resonators as one class of micromachined resonators. After that, the methods to improve the performance of such resonators are discussed and evaluated by the results from the finite element model (FEM) simulations. The work done to deposit UNCD films with optimum characteristics for fabricating high frequency resonators and also the fabrication process flow of the TPoS resonators are explained in chapter 4. Chapter 5 presents the experimental results from the resonator designs with various geometries and different configurations. In addition, a resonator design with a record low insertion loss at 900 MHz and low TCF value is demonstrated. Lastly, the accomplishments in the thesis are summarized and the future research is pointed out in chapter 6.

CHAPTER 2

REVIEW OF LITERATURE

One of the most substantial parts of the emerging communication systems is resonator that is needed for building filters, oscillators, mixers, sensors, etc. The resonators have to have a high quality factor, good stability, low insertion loss, high power handling capability, small size, and low power consumption. Microelectromechanical systems (MEMS) have become a promising technology for providing low-cost, small-size and high-performance solutions for radio frequency applications. However, there is still a high demand for devices that are compatible enough to be integrated on-chip along with other CMOS components to further miniaturize the RF systems.

There are two main transduction methods that have been developed to build on-chip micromachined resonators: electrostatic and piezoelectric. Resonators with very high quality factors based on electrostatic actuation mechanism have been developed, but these resonators suffer from large motional impedances (at least few kΩ), which increases at higher resonance frequencies, preventing them from direct interfacing to standard 50 Ω electronics [1, 2, 3]. In order to compensate for such large motional impedances, DC bias voltages higher than values allowed in IC technologies are required [4]. In addition, reaching high frequencies using this technology requires very small gaps (few tens of nanometers) between the resonator and the

electrodes which complicates the fabrication process [5]. Plus, the capacitive resonators exhibit poor linearity, especially at higher frequencies where the gap is reduced.

On the other hand, piezoelectric materials offer larger electromechanical coupling coefficient relative to that of electrostatic transduction, which plays an important role in achieving small motional impedance for resonators. Film bulk acoustic resonators have been demonstrated with high quality factors and high coupling coefficients suitable for building filters with large bandwidths [6, 7], but since film bulk acoustic resonators (FBAR) operate in the thickness-mode, the drawback is the limitation on frequency variation on one single substrate. While lateral-extensional piezoelectric resonators benefit from relatively large electromechanical coupling coefficient of piezoelectric transduction, they also offer a wide range of frequencies on a single substrate. Such piezoelectric resonators have been reported with high quality factors and resonance frequencies in the range of tens of KHz to few GHz [8, 9, 10, 11]. The lateral-extensional piezoelectric resonators can be classified into two groups: with and without substrate. Thin-film piezoelectric-on-substrate (TPoS) resonators exhibit better power handling capability and yield compared to lateral-extensional resonators without substrate [12].

Materials with high energy density, low dissipation, high acoustic velocity, and low temperature coefficient of frequency are desired as the substrate for fabricating TPoS resonators. In recent years, the MEMS community has found interest in using diamond instead of silicon as the substrate due to the advantages it offers. Some of these advantages are the high Young's modulus, bio-compatibility, low wear-rate, low dissipation properties, etc. Because of its high Young's modulus (YM), diamond has a great potential to extend the frequency above the limits achievable by silicon (up to 2x increase in frequency) [13, 14, 15]. In this work, ultrananocrystalline diamond was used to build thin-film piezoelectric-on-diamond (TPoD) resonators.

A TPoS resonator is fabricated on both silicon and three UNCD substrates with Young's modulus of 491GPa, 650GPa, and 933GPa showing up to 2x increase in the resonance frequency. This work also studies the effect of lateral dimensions and support configuration on the resonator's performance using finite element model (FEM) simulation in COMSOL and results will be compared with the actual measurements. Also, methods to optimize the performance of the thin-film piezoelectric-on-diamond resonators will be discussed. A ~900MHz TPoD resonator with record low insertion loss value of 2.6dB is reported, and the power handling capability and the temperature dependency of the frequency of this resonator are examined.

CHAPTER 3

METHODOLOGY

This chapter begins with an introduction to thin-film piezoelectric-on-substrate (TPoS) resonators as one class of micro-machined piezoelectric resonators. The concept of operation is explained. Then, the methods to optimize the performance of such resonators are discussed followed by FEM simulations for better understanding and also verifying the proposed ideas.

3.1 THIN-FILM PIEZOELECTRIC-ON-SUBSTRATE RESONATOR

TPoS resonators are comprised of a piezoelectric material deposited on a substrate with low acoustic loss, high acoustic velocity, and high energy density. The piezoelectric layer is sandwiched between two metal layers and is actuated by the electric field applied through the input electrode(s) and the bottom ground layer (Figure 1). The applied electric field produces a stress field (Figure 2) in the piezoelectric layer which is consequently induced in the substrate underneath. The generated electric charge due to the piezoelectric effect is then harvested from the output electrode(s). The TPoS resonator is intended to vibrate along the width of the structure; however, there is also some vibrations along the length due to Poisson coefficient. The resonance

frequency of the resonator depends on the order of the resonance harmonic and the finger pitch which is defined as the center-to-center distance of two adjacent electrodes. As is shown in the mode shapes brought in Figure 2, the wavelength for the first harmonic is equal to 2x the width of the device; where for the third harmonic, the half-wavelength is equal to the finger pitch.

In the following, the focus is on the resonance frequency of the maximum order harmonic that can be excited in the structure without any charge cancelation due to electrode configuration or in simpler words, the number of electrode fingers on top of the resonator structure e.g. the resonator shown in Figure 1 is called a 3rd order harmonic resonator.
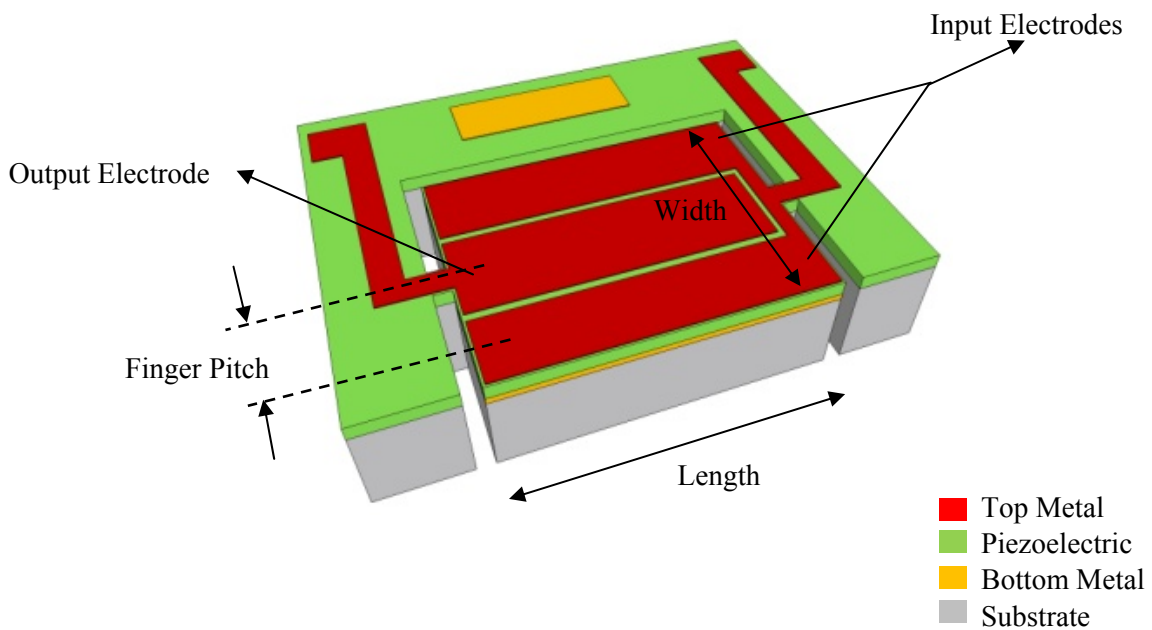
Figure 1- 3D structure of a third order harmonic thin-film piezoelectric-on-substrate resonator with three electrode fingers and a pair of support tethers.
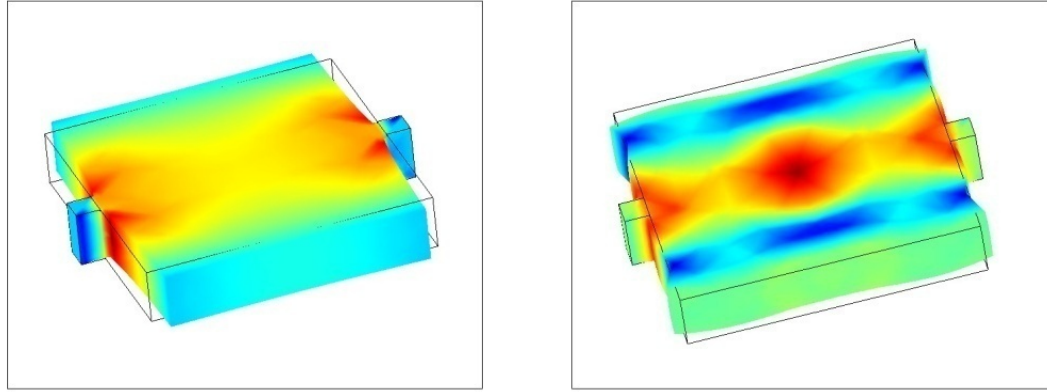
Figure 2- Mode shapes for first order (left) and third order (right) harmonics of the TPoS resonator showing the stress field in the substrate. The areas in red are under tensile stress and areas in blue have compressive stress.

3.2 PERFORMENCE OPTIMIZATION OF TPOS RESONATOR

As in any non-ideal system, there are inherent loss mechanisms in piezoelectric transformation, hence, not all of the applied energy is confined in the resonator structure at resonance. Part of this energy is transferred to the rest of the substrate as the acoustic wave travels through the support tethers. Another portion of the energy is lost due to the electrical resistivity of the metal electrodes and the contacts. A small portion of the applied energy is transformed to heat as the structure vibrates, which is usually denoted as the material damping or thermoelastic loss. Plus, there is air damping, which is present when the resonator operates in air and is inversely proportional to frequency. In this work the targeted frequencies are in the range of 400MHz-1.2GHz. In this range the more dominant loss mechanisms are the electrical and the support loss.

In order to study and improve the performance of the TPoS resonators, a finite element model (FEM) was developed that includes the electrical and the support loss as the two dominant sources of loss [16]. The support loss is considered by embedding a perfect matching layer (PML)

8

in the model to completely absorb the acoustic wave escaping through the tethers, impinging on the PML. The electrical loss is modeled by assuming finite electrical resistivity for the metal electrodes (Figure 3-a). By taking advantage of the symmetry in the resonator structure, only half of the structure is simulated to be able to perform the simulations in a reasonable time. Using this model, the resonance frequency and the frequency response of the resonator can be predicted. In all the simulations carried out in this thesis, the Young's modulus of the substrate is set to 650GPa which is the actual Young's modulus of one of the diamond wafers used for fabricating TPoD resonators. The simulated frequency response of a 7th order harmonic TPoD resonator is depicted in Figure 3-b. The insets show the spurious mode shapes close to the resonance mode. These spurs which are intrinsic to any resonant structure have to be suppressed by design. Adding more tethers to the structure is one way to eliminate the spurs, while it also increases the quality factor of the resonator [9].

Three 7th order harmonic TPoD resonators with different number of tethers were simulated for comparison and results are brought in Figure 4. The increase in the resonance frequency of the device is due to the added stiffness caused by adding tethers to the structure. The insertion loss and quality factor of the design with two pairs of tethers has improved compared to the design with only one pair of tethers. The author believes that this is due to the refinement of energy into the desired resonance mode by bounding the structure to resonate in the target mode-shape and preventing the an-harmonic mode-coupling. But this trend is not maintained as the number of tether pairs is increased to three. This is because the acoustic energy escaping the resonator structure increases by increasing the number of tethers and this increase will not be fully compensated by the added restraint. So, the design with three pairs of tethers has a larger IL relative to two-tethered design but has no strong spurs in a 20 MHz vicinity of the resonance frequency.

Finger Pitch: 8μm
Device Length: 52μm
Support Width: 6μm
Diamond Thickness: 3μm
AlN Thickness: 0.5μm

PML

(a)

(b)
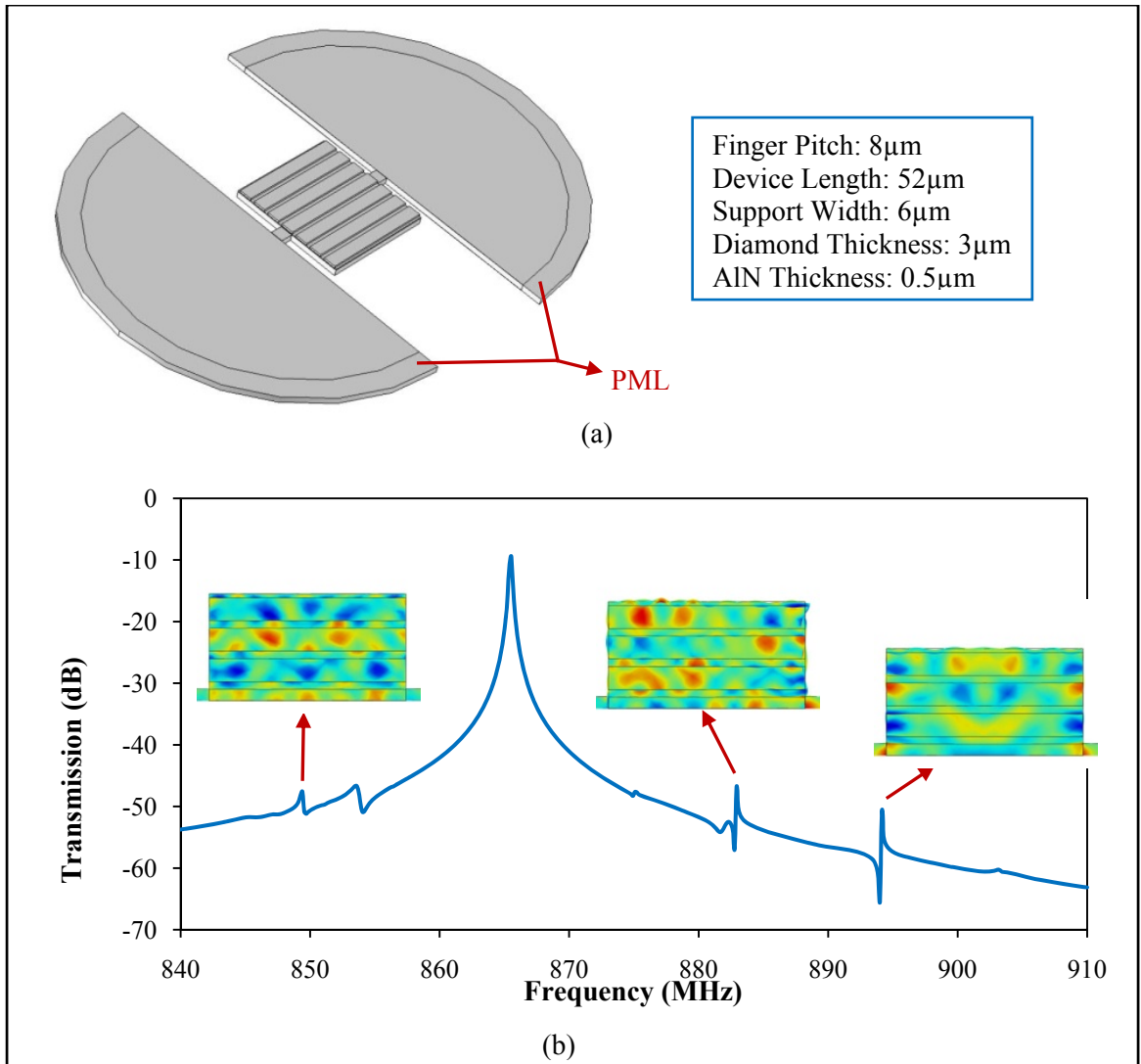
Figure 3- (a) FEM model for a 7th order harmonic TPoD resonator with one pair of support tethers. (b) Simulated frequency response for the 7th order harmonic TPoD resonator showing the mode shape of the half-device for the desired resonance peak and the nearby spurious modes.
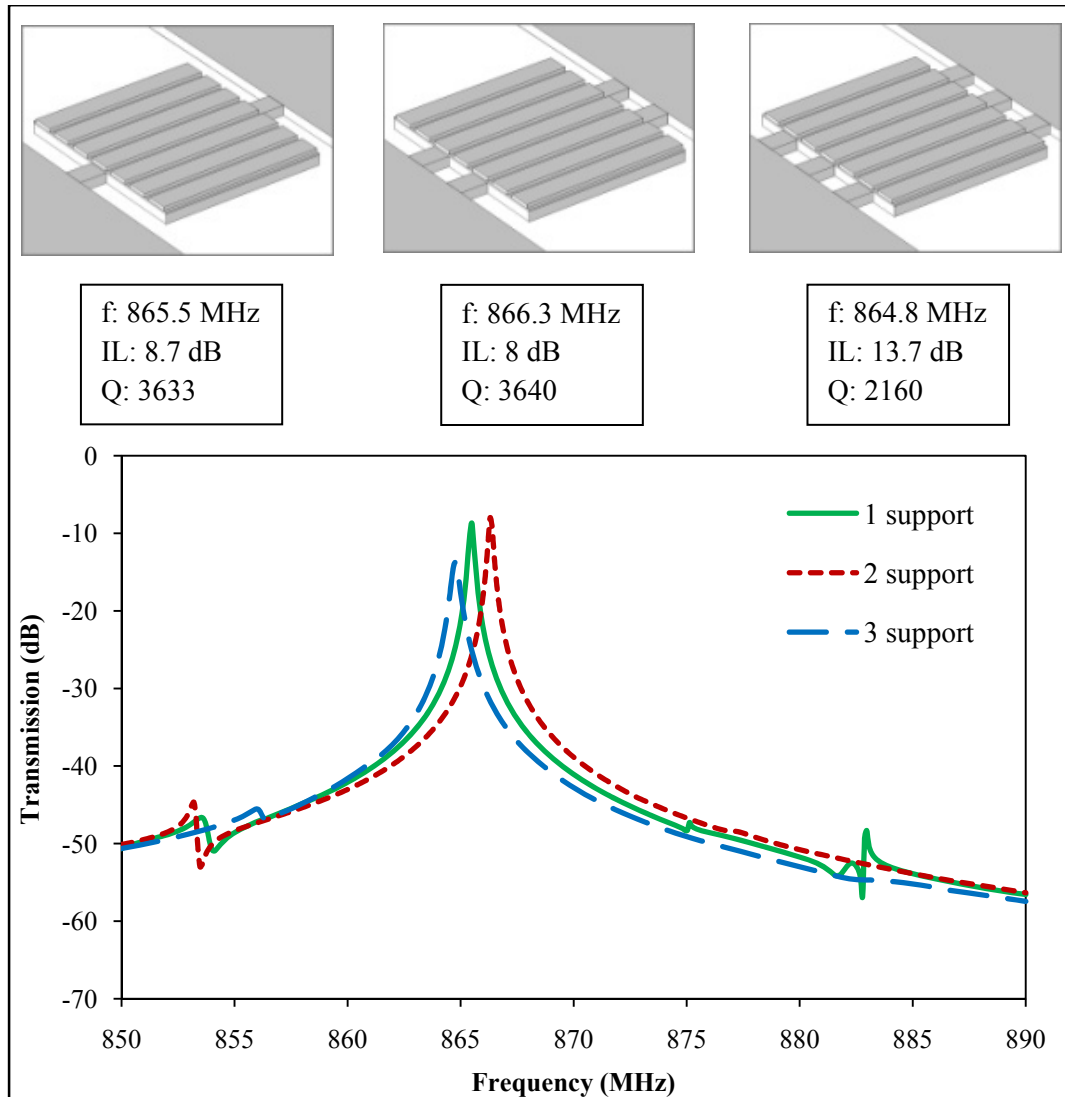
Figure 4- Simulated frequency responses for 7th order harmonic TPoD resonators with one, two, and three pairs of support tethers showing the effect on the insertion loss and the quality factor of the resonator.

As explicitly explained in [16], the tether length alters the performance of the resonator by changing the acoustic impedance seen by the wave traveling from the resonator to the substrate through the support tethers.

In order to reduce the insertion loss of the lateral-extensional resonators, the motional impedance of the resonator has to be decreased. This can be done by increasing the actuation area on the

11

resonator by increasing the lateral dimensions of the structure. So, one approach is to increase the length of the resonator. Figure 5 represents the frequency responses for the aforementioned 7th order harmonic TPoD resonator with different lengths. By increasing the length from 48μm to 52μm, the insertion loss has improved by 3 dB and also the close-to-resonance spur no longer exists for the 52μm long design. But as the length is further increased to 56μm, a sharp unwanted peak appears very close to the target resonance frequency. Besides, the number of spurious modes increases for the longer structures. This issue can be resolved to some extent by adding support tethers to the structure. As the length is increased, the resonance frequency decreases which is due to the loosening effect associated with larger structures. Figure 6 shows the dependency of the quality factor and the insertion loss of the lateral-extensional resonator on the aspect ratio of the design, with the aspect ratio defined as the ratio of the length to the width of the resonator. In these simulations the width of the device is kept constant and the length has been increased. Rectangular markers indicate the lengths which are equal to odd multiples of half-wavelength, while triangular markers are the $(2n + 1) * \lambda/4$ long designs, and the circle ones signify the designs with lengths equal to $(2n + 1) * \lambda/8$. The results show that by continually increasing the length, the IL and Q would not improve constantly. In fact, for the lengths equal to odd multiples of $\lambda/8$, both the IL and Q deteriorate. Whereas odd multiples of $\lambda/2$ and $\lambda/4$ seem to have lower IL and higher Q values. It has to be remembered that even though for longer lengths, the IL and Q improve on average but the frequency response is not as clean as it is for shorter lengths because of the existence of spurious modes.

The other method to increase the actuation area on the resonator is to excite the resonator in higher order harmonics. In other words, increase the number of the fingers by repeating the structure along the width [15].

Based on the simulation data shown in the above figures, the optimum design would have support length of $(2n+1)^\lambda/_8$ and a length equal to $(2n+1) * ^\lambda/_2$. Depending on the desired characteristics, there is an optimum aspect ratio for the lateral dimensions of the resonator.
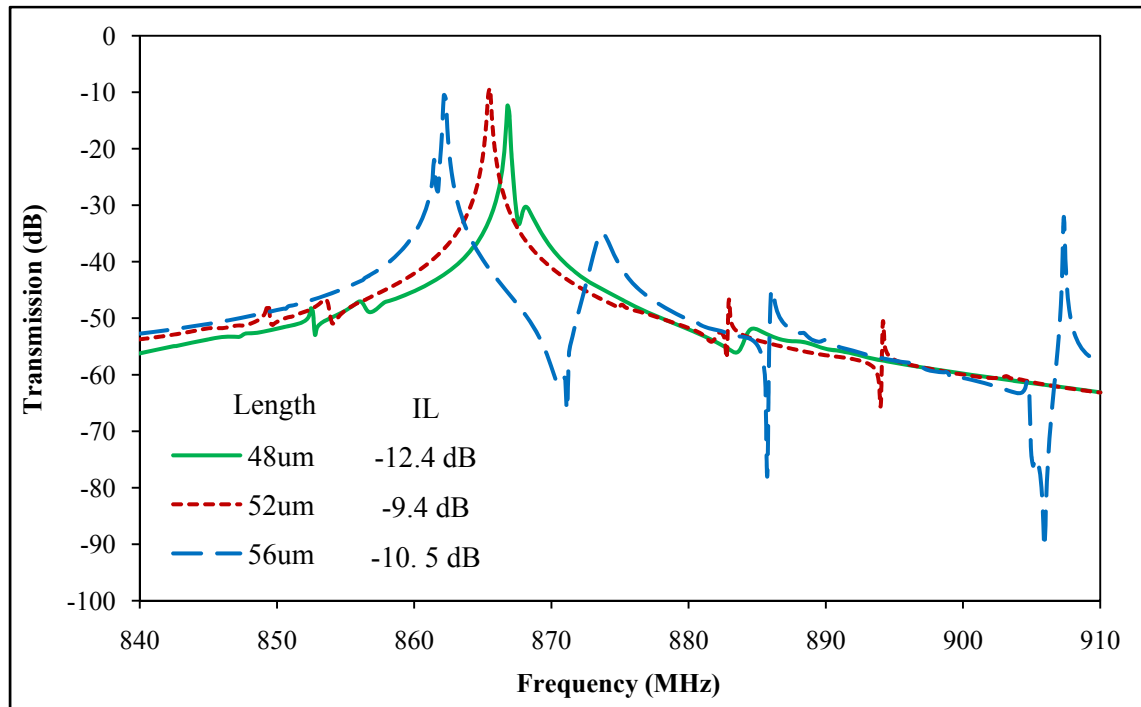
Figure 5- Simulated frequency responses of a 7th order harmonic TPoD resonator with one pair of tethers and different lengths. The spurs for the 56µm long design are circled in blue.
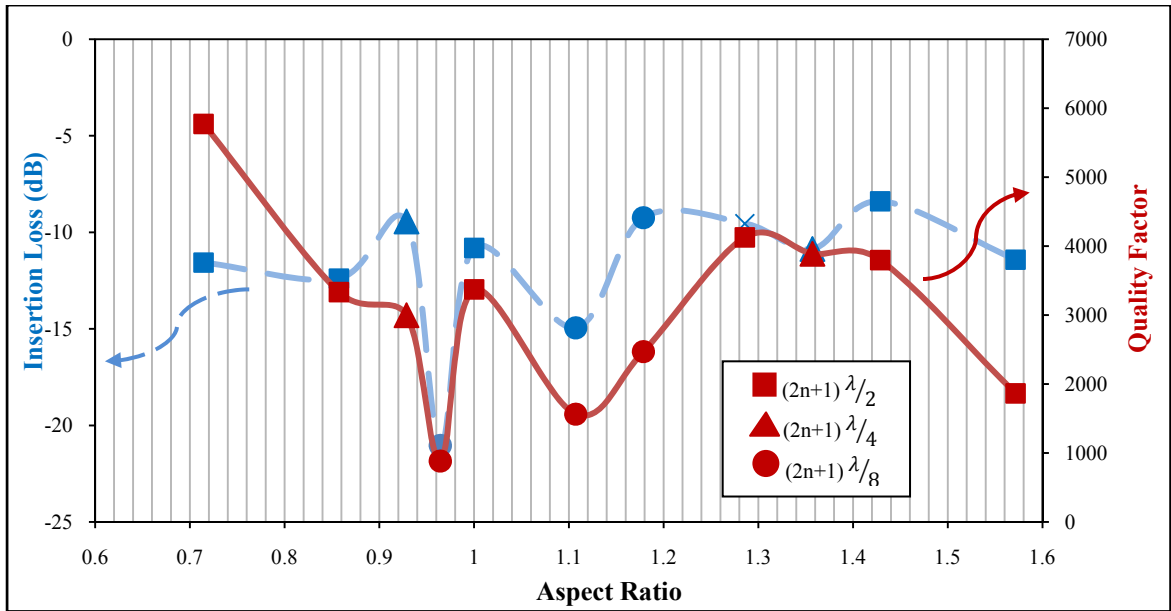
Figure 6- Dependency of the insertion loss and quality factor of a 7th order harmonic TPoD resonator on the aspect ratio of the structure showing an overall improvement in the insertion loss and quality factor as the length is increased while the width is fixed.

CHAPTER 4

FABRICATION

This chapter describes the work to optimize the properties of the ultrananocrystalline diamond (UNCD) films used to make the thin-film piezoelectric-on-diamond (TPoD) devices as well as the integration of high-quality AlN films on smooth (~1 nm rms roughness) UNCD films achieved via wafer-scale polishing. After that the process for fabrication of TPoD resonators will be discussed.

4.1 PREPARATION OF UNCD FILMS

Diamond has gained much popularity in MEMS community essentially due to its high Young's modulus and low dissipation properties [17]. Thin-film piezoelectric-on-diamond (TPoD) bulk-lateral-mode resonators with 80% higher frequency compared to the same devices fabricated on silicon have shown much promise in scaling the resonance frequency beyond the limits achievable by silicon [14, 15]. However, the orientation of the piezoelectric film is critical to retain the low insertion loss performance of the resonators. In the earlier work, a polished oxide layer had to be deposited on the nanocrystalline diamond substrate to promote the growth of a

highly-oriented piezoelectric film on the rough surface of the substrate [14]. As can be seen in Figure 7, the surface of the ZnO deposited on oxide is much smoother than the one directly deposited on nanocrystalline diamond leading to a better film quality and hence, a higher coupling coefficient. This oxide layer also helps reduce the TCF of the resonator [18]. This was the bottleneck for realization of very high frequency resonators since the presence of the oxide would significantly alter the mode shape and lower the quality factor and the frequency. As depicted in the mode shapes of Figure 8, the resonance frequency has decreased by 15% and the displacement is distorted for the design with the buffer oxide layer [14].

In this work the surface roughness of diamond substrate is substantially reduced by depositing ultrananocrystalline diamond (UNCD) followed by standard chemical mechanical planarization (CMP) process. Such smooth surfaces allow for direct sputtering of metal/ piezoelectric/ metal heterostructures with a large coupling coefficient that enable monolithic integration of dispersed-frequency resonators.

(a)   (b)
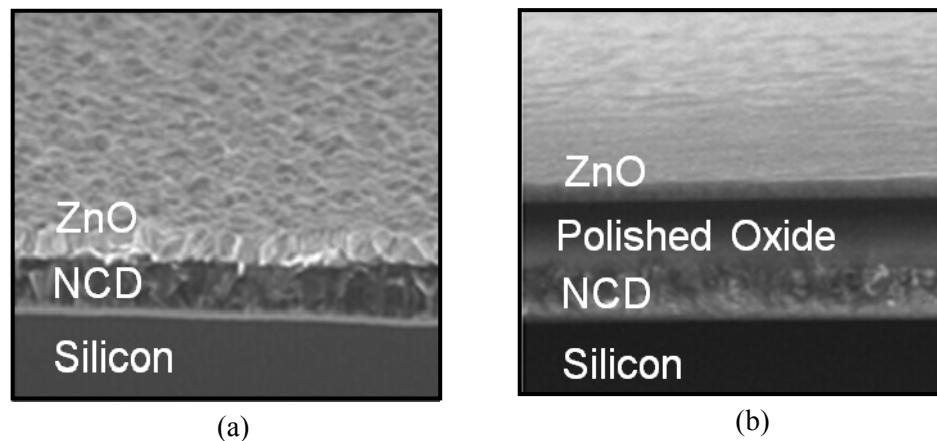
Figure 7- (a) ZnO directly sputtered on nanocrystalline diamond, (b) Polished oxide was deposited as a buffer layer before the deposition of ZnO [14].
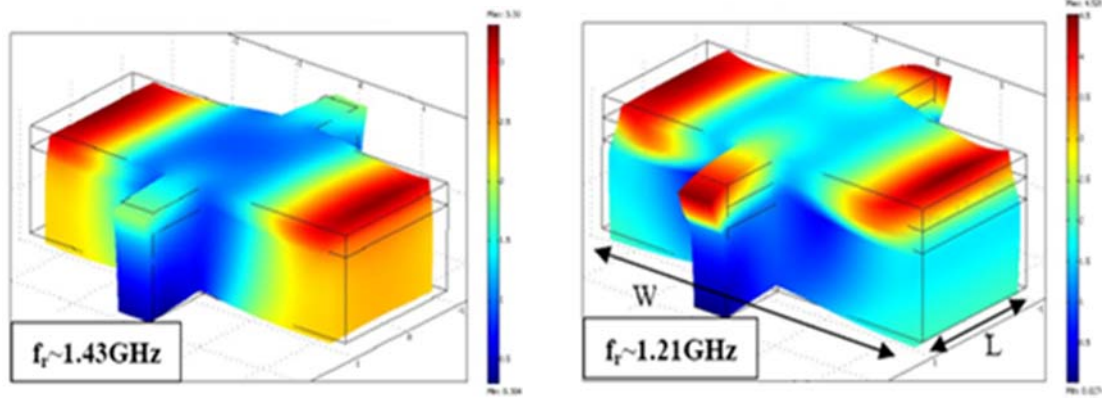
Figure 8- Effect of buffer oxide layer on the frequency and mode-shape of the lateral-extensional resonator [14]. The mode-shape on the left represents the device without the buffer oxide layer while the figure on right represents the design with an oxide layer.

The acoustic velocity is a function of Young's modulus (E) and mass density (ρ) as follows:

$$\alpha = \sqrt{E/\rho} \qquad (1)$$

where α symbolizes the acoustic velocity. Since the frequency of a resonator built on a diamond substrate is directly proportional to α of the diamond, it is critical that the Young's modulus of the UNCD be consistently high and uniform across the wafer.

Standard UNCD films have Young's modulus from 650 GPa to 750 GPa, yielding up to 1.6 times increase in frequency compared to silicon-based devices designed with the same lateral dimensions. The challenge in increasing the modulus closer to the largest theoretical value possible (~1200 GPa) is maintaining as small of a grain size as possible to retain the as-deposited smoothness of the material so that CMP-processing is still capable of reducing the rms roughness to about 1 nm.

Three diamond substrates with different Young's modulus were prepared to fabricate TPoD resonators. Ultrananocrystalline diamond (UNCD) was deposited using hot filament chemical

vapor deposition (HFCVD) technique. The very small size of the UNCD grains warrant very smooth surfaces which allow for the deposition of highly oriented piezoelectric thin films e. g. AlN. In order to increase the Young's modulus of the diamond films close to the theoretical values, the deposition temperature was increased from 660 ºC to 810 ºC by increasing the temperature of the filaments [15]. Figure 9 shows the dependency of the Young's modulus on the filament temperature as well as the film thickness. Increasing the deposition temperature also reduces the residual stress in the film from 300-400 MPa compressive to about 100 MPa tensile even for films as thick as 5-6 microns which is more desirable for deposition of the metal/ piezoelectric/ metal stack and the operation of TPoS devices. However, the average grain size of UNCD films grows at higher temperatures, resulting in films with rougher surfaces with rms roughness values around 60 nm rms as presented by AFM data in Figure 10-a. Such high rms roughness values make the integration of high quality AlN films on the diamond very challenging due to the crystallographic orientation disorder that occurs at the AlN/diamond interface. A highly disordered AlN film results in very poor average piezoelectric coefficient and therefore an inferior insertion loss (IL) for the resonators. This issue was resolved by adding an additional polishing step during which a more aggressive slurry and a greater applied force was used initially to bring the roughness down to about 15 nm, after which the conventional chemical mechanical polishing (CMP) process was performed to further reduce the roughness to less than 1nm (Figure 10-b). The characteristics of the three UNCD wafers are listed in Table 1.

Table 1- Characteristics of the diamond films used for fabrication of TPoD resonators.

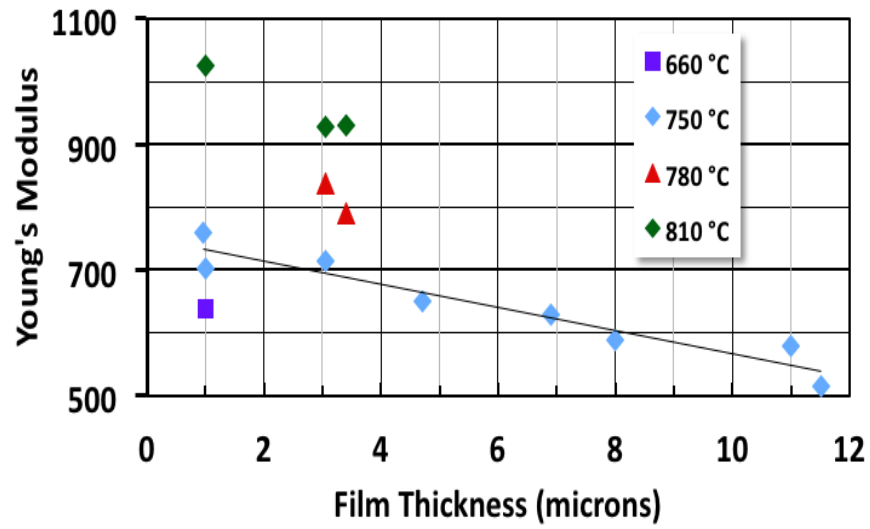| Wafer	UNCD Thickness (μm)	Young's Modulus (GPa)	Surface Roughness (nm)	AlN Thickness (μm)	AlN FWHM
A	~3	491	0.4-0.5	0.5	4.07°
B	~3	650	0.4-0.5	0.5	3.05°
C	~3	933	1.0-1.8	0.5	3.19°

Figure 9- Dependency of the Young's modulus of the UNCD film on the deposition temperature.

(a)

(b)
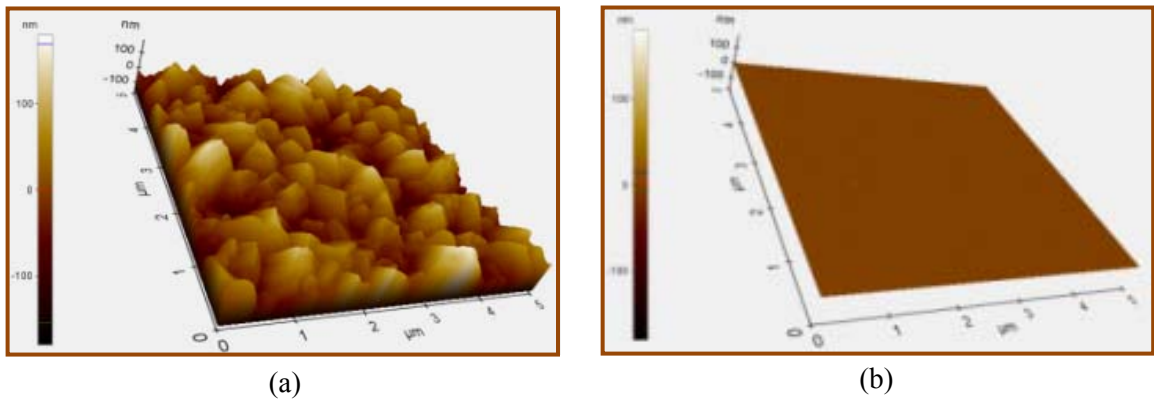
Figure 10- AFM image of high Young's modulus (950 GPa) diamond film surface (a) before and

(b) after CMP showing less than 1nm final rms roughness.

4.2 FABRICATION PROCESS

After UNCD deposition and polishing, the stack of Mo (100 nm)/ AlN (500 nm)/ Mo (100 nm) was sputtered (Figure 11). AluminumNitride (AlN) is used as the piezoelectric layer due to superior process compatibility, relatively high acoustic velocity and high electrical resistivity. Molybdenum is chosen as the metal layer because it has a small lattice and thermal expansion coefficient mismatch with AlN in addition to low acoustic-loss.

The two-dimensional X-ray diffraction frames from AlN film deposited on both polished and unpolished diamond is displayed in Figure 12 for comparison. The brighter the X-ray rings, the denser is the diffraction at a certain angle which means that the grains are more aligned in that specific angle. The polished diamond exhibits a higher intensity at specific values of chi that confirms the existence of highly textured AlN. Figure 13 shows a SEM from the smooth surface of the AlN sputtered on polished UNCD compared to the rough surface of ZnO deposited on NCD in Figure 7. Figure 14 represents the X-ray rocking curve of the deposited AlN film with a full-width half maximum (FWHM) of about 3 degrees. The quality of the film was very close to that of the c-axis aligned AlN deposited on polished single crystal silicon substrates for which the typical FWHM is in the range of 2.0°-2.5º.
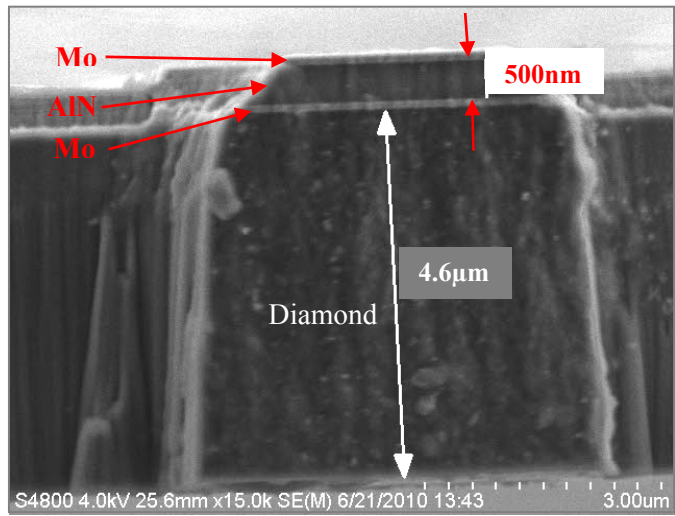
Figure 11- Cross-section of a broken device showing the stack of Mo/AlN/Mo directly sputtered on UNCD.
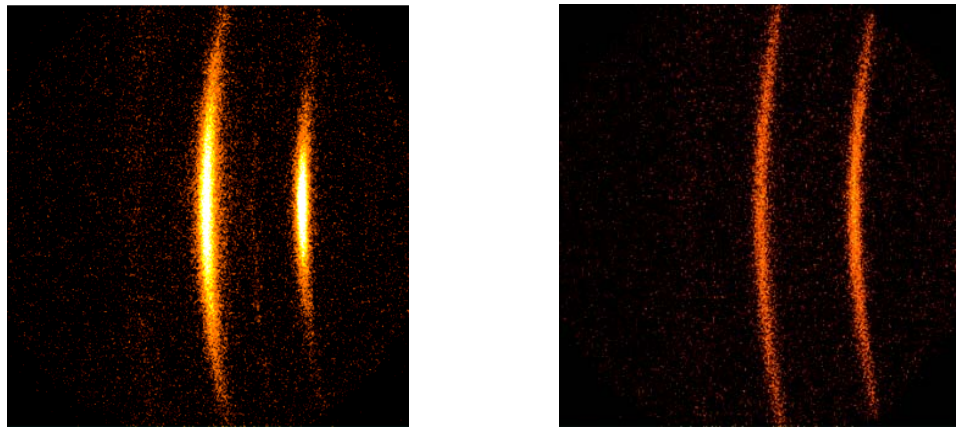
Figure 12- 2-D XRD frames for polished diamond (a) and unpolished diamond (b).
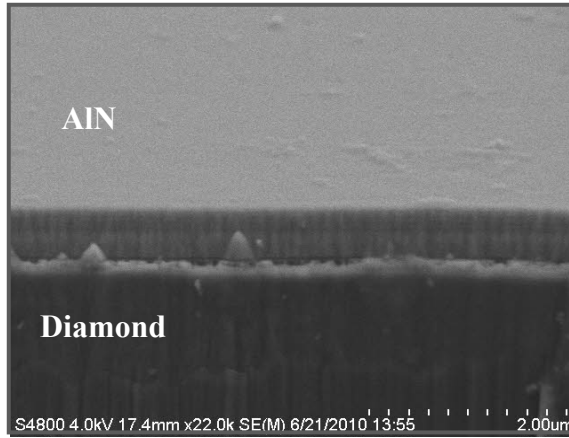
Figure 13-SEM of the smooth surface of AluminumNitride sputtered on polished UNCD.

FWHM: ~3°
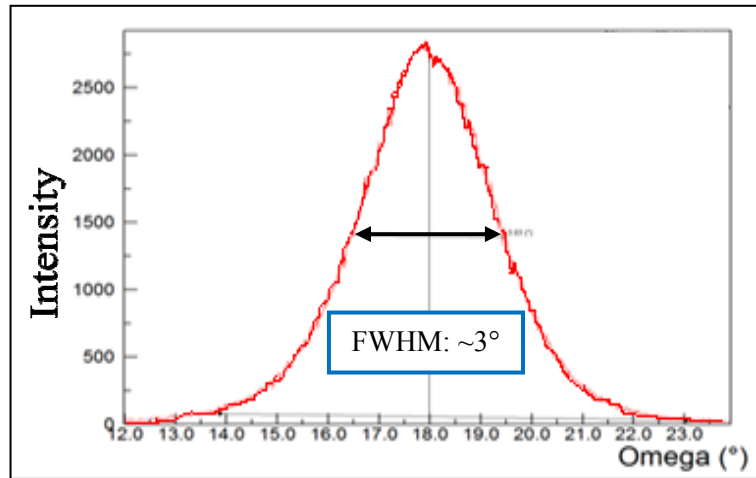
Figure 14- Rocking curve of the AlN film deposited on UNCD film with FWHM of 3°.

The schematic flow diagram of the fabrication process is shown in Figure 15. After depositing UNCD film and the bottom metal layer on the polished surface of the silicon wafer, the bottom metal is patterned by dry-etching in   and   plasma to remove the areas underneath the pads and tracks in order to reduce the parasitic capacitances (Figure 15-a). Then the AlN and the top metal layers are sputtered followed by patterning the top metal (during the same process as the bottom metal) to form the top electrodes (Figure 15-b). Then the AlN is wet-etched in a Tetramethylammonium hydroxide (TMAH) solution at   to create access to the bottom metal

(Figure 15-c). In order to improve the electrical contact and reduce the ohmic losses of the metallic pads and the contact areas, a layer of gold (100-200 nm) is sputtered. However, gold alone can undergo de-lamination; a layer of chromium is therefore used for improved binding strength (Figure 15-d). The device stack is then etched down to the Si substrate in an inductively coupled plasma etcher (AlN in Cl_2 and Diamond in O_2/CF_4 plasma) as shown in Figure 15-e. Finally, devices are released by dry etching silicon from the backside in a deep reactive ion etching chamber (Figure 15-f).
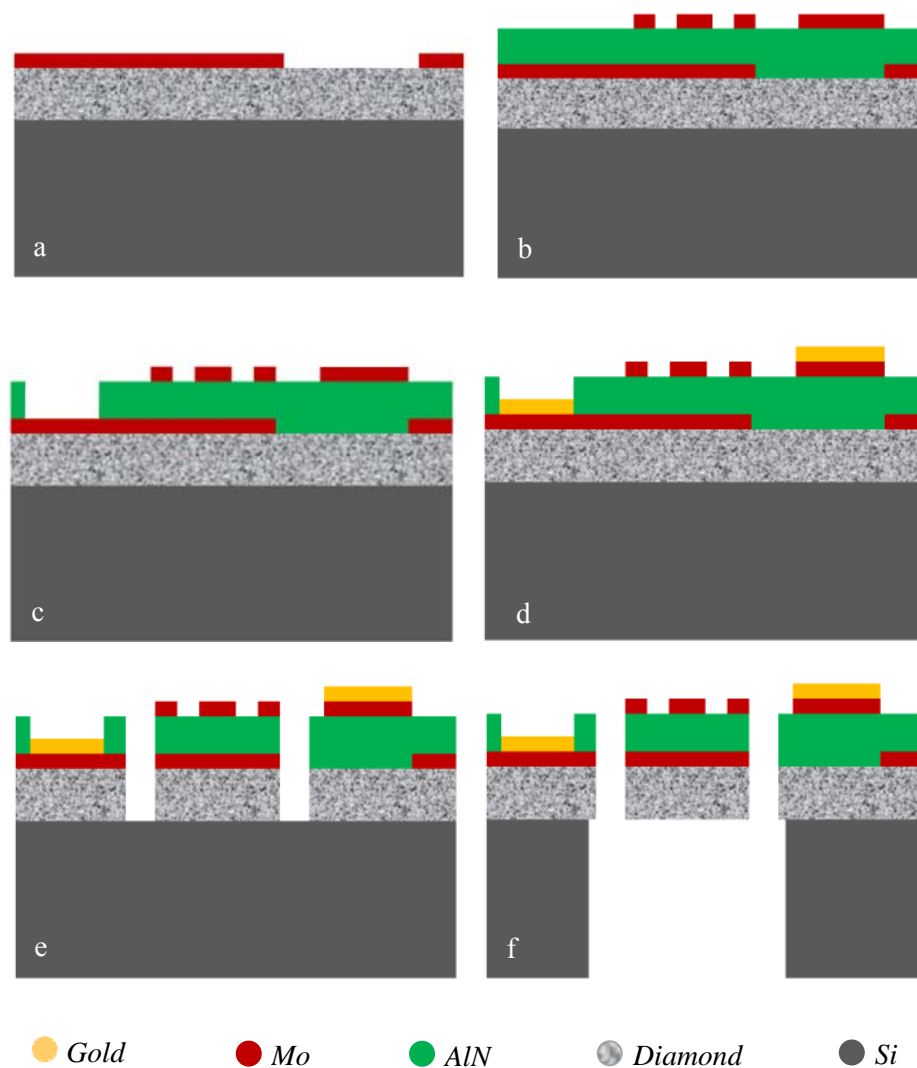
Figure 15- Fabrication process flow: (a) Patterning the bottom metal layer, (b) Deposition of AlN and top metal layer, followed by patterning the top metal, (c) Wet-etching the AlN to gain access

to the bottom metal, (d) Sputtering gold on the contact areas, (e) Etching the stack (f) followed by

releasing the device by etching the handle silicon from the backside.

CHAPTER 5

EXPERIMENTAL RESULTS

After fabricating the diamond wafers, the S-parameters of the devices were measured using a two-port Agilent E8358A Network Analyzer and a pair of GSG probes while terminated with the internal 50Ω impedance of the network analyzer. All the measurements in this section were carried out at atmospheric pressure and ambient temperature, except for measurement of the temperature coefficient of frequency (TCF) which was performed in a vacuum probe station. Prior to all the measurements, short-open-load-thru (SOLT) calibration was performed on a reference substrate.

5.1 CHARACTRIZING UNCD FILMS

To characterize the quality of the UNCD films, a multi-tethered 21st order harmonic resonator was fabricated on the three diamond substrates mentioned in section 4.1 and also on a 5µm thick silicon-on-insulator (SOI) substrate. The transmission responses are plotted in Figure 16 along with the SEM of devices fabricated on both silicon and diamond. The diamond thickness is ~3 µm for all the three substrates whereas the silicon thickness is 5 µm. Considering the $f.Q$ product
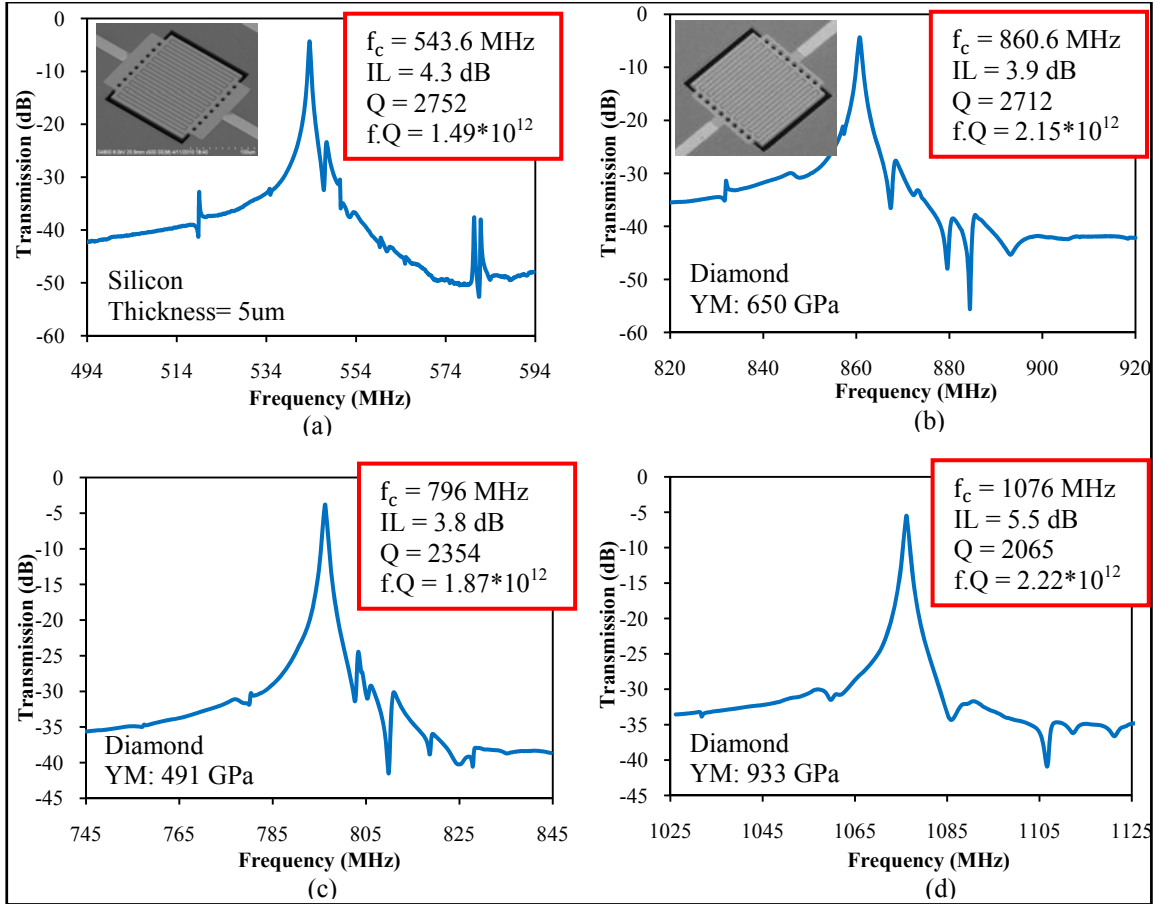
Figure 16- Frequency response of a multi-tethered 21st order harmonic TPoS resonator fabricated on (a) silicon, (b) UNCD with YM of 650 GPa, (c) UNCD with YM of 491 GPa, and (d) UNCD with YM of 933 GPa.

as the figure of merit for resonators, devices fabricated on diamond show up to 1.5 times improvement compared to the device fabricated on silicon.

5.2 OPTIMIZATION

FEM simulation helps identifying how different parameters affect the performance of the TPoS resonators but for any desired characteristics there is an optimum configuration which cannot be absolutely designed using the FEM model in a timely manner. To verify the accuracy of the

simulation results in chapter 2, 21st order harmonic resonators with different lengths, number of fingers and number of supports were designed and fabricated on the UNCD substrate.

Figure 17 shows the best results for a 21st order harmonic TPoD resonator with different number of support tethers fabricated on the UNCD substrate with Young's modulus of 933GPa. These results confirm that by adding tethers to the structure, the insertion loss and quality factors can be improved along with the reduction in the number and the strength of the spurious modes as circled in the figure. But unlike the simulation results of Figure 4, the resonance frequency of the resonator does not increase constantly as the number of supports is increased. This is due to the fact that the UNCD thickness is not perfectly uniform across the wafer; hence, the equivalent Young's modulus of the AlN/diamond stack varies on the wafer. Figure 18 demonstrates the

Figure 17- Best measured results on the diamond substrate with 933GPa Young's modulus for a 21st order harmonic TPoD resonator with 5, 9, and 11 pairs of tethers showing how adding tethers to the resonator structure improves the quality factor and insertion loss of the resonator.
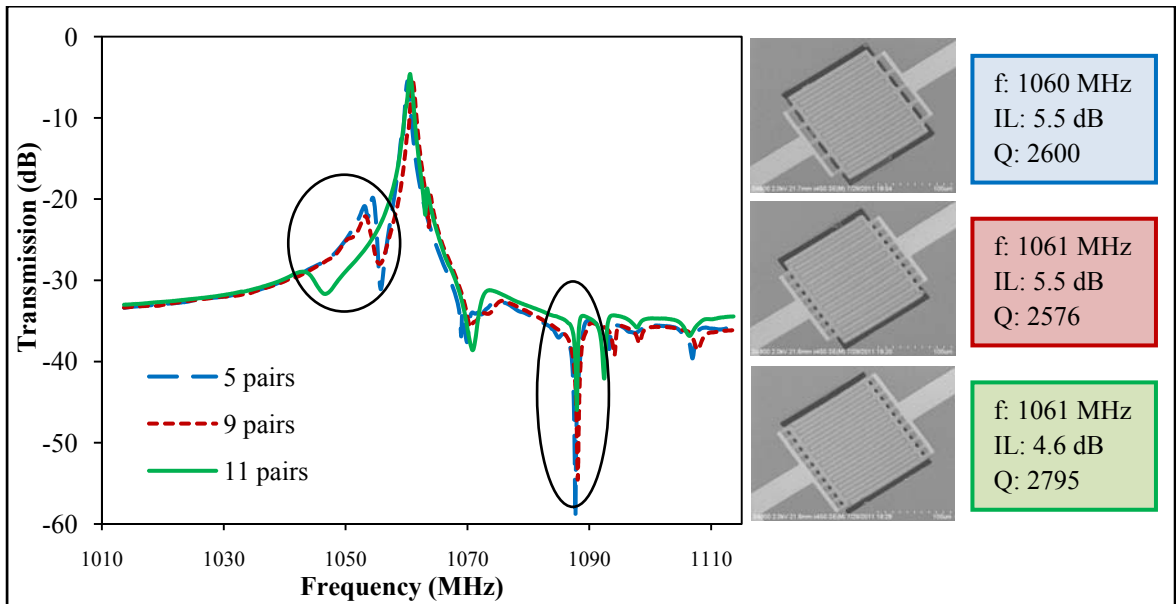
results from the fabricated resonators on one UNCD substrate and the average quality factor and insertion loss. As can be seen, both the average insertion loss and the average quality factor improve as the number of tethers is increased.
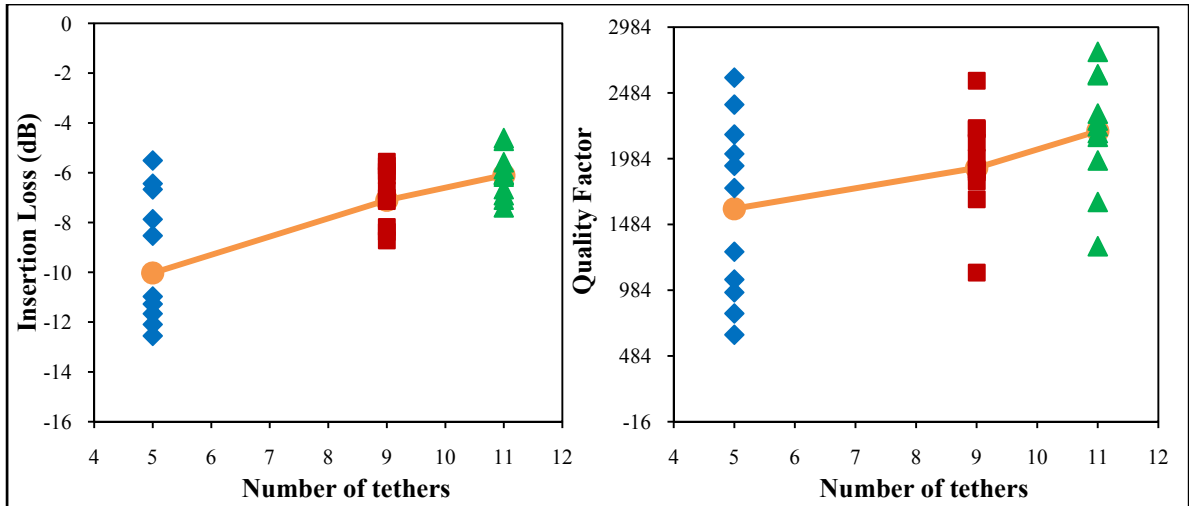
Figure 18- Measurement results from 21st order harmonic resonators with 5, 9, and 11 pairs of tethers all around the fabricated wafer with YM of 933 GPa showing an overall improvement on IL and Q as the number of support tethers is increased.

Based on the simulation results previously presented in Figure 6, both odd multiples of $\lambda/2$ and $\lambda/4$ seem to be a more suitable choice for the length of the TPoD resonator. Therefore, to study the effect of length on the resonator performance, 21st order harmonic resonators with various lengths equal to $(2n + 1) * \lambda/2$ and $(2n + 1) * \lambda/4$ were designed and fabricated. Data presented in Figure 19 is collected from devices all over the wafer with lengths equal to 136.8 μm, 147.6 μm, 151.2 μm, 169.2 μm, 180 μm, and 198 μm. The corresponding aspect ratios and the relation with the wavelength are listed in Table 2. As the length is increased from ~136.8 μm to ~151.2 μm, the average insertion loss of the resonators reduces, but there is a relatively large increase in the insertion loss for 169 μm long designs. Again, by further increasing the length, insertion loss of the resonators is improved on average. For the longer designs even though the IL is lower but

this is achieved at the expense of having more spurious modes in the close vicinity of the resonance frequency.

Table 2- Different lengths for the fabricated 21st order harmonic TPoD resonators and the corresponding aspect ratios.

Length (µm)	136.8	147.6	151.2	169.2	180	198
	19*λ/2	41*λ/4	21*λ/2	47*λ/4	25*λ/2	55*λ/4
Aspect Ratio	0.9	0.97	1	1.12	1.19	1.3

As noted before, by repeating the structure along the width, the actuation area can be increased. This time, 133.2 µm long resonators were designed to actuate different resonance harmonics at a certain resonance frequency. The average values of the quality factor and the insertion loss were calculated after ignoring the inapplicable data points (Figure 20). The average quality factor increases as the number of fingers is increased until it reaches a maximum, but the average insertion loss does not follow the same pattern and has a minimum for the resonator with 29 fingers. Again, for a fixed length there seems to be an optimum order harmonic where the quality factor is maximum and the insertion loss is minimum. According to Figure 20, for the 133.2µm long resonator, the 29th order harmonic (for which the aspect ratio is ~1.6) seems to be the optimum point with the lowest insertion loss and the maximum quality factor.
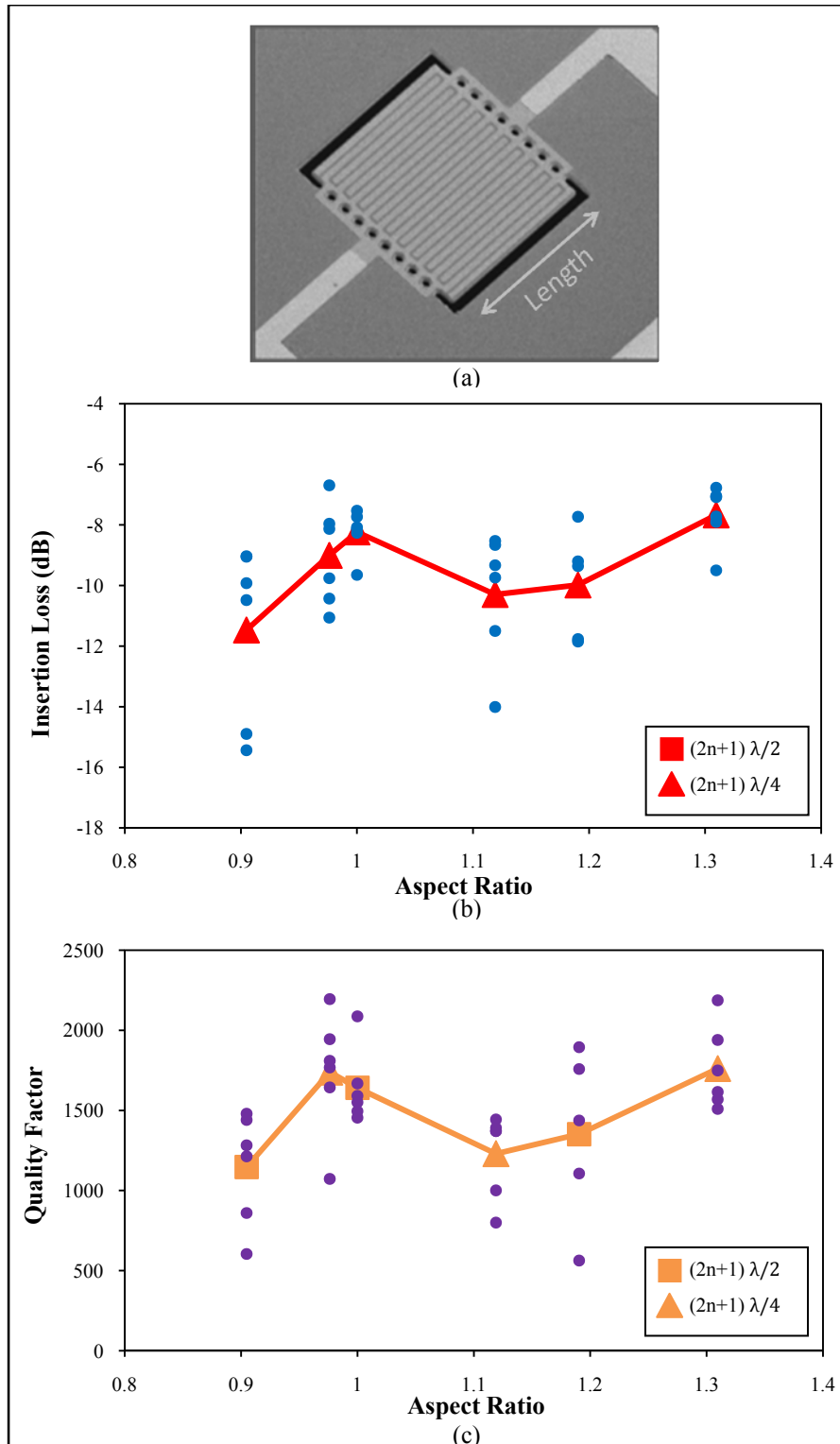
Figure 19- (a) SEM of a 21st order harmonic multi-support TPoD resonator, (b) Dependency of the insertion loss on the length of the fabricated resonators, and (c) dependency of the quality factor of the resonators on the length.
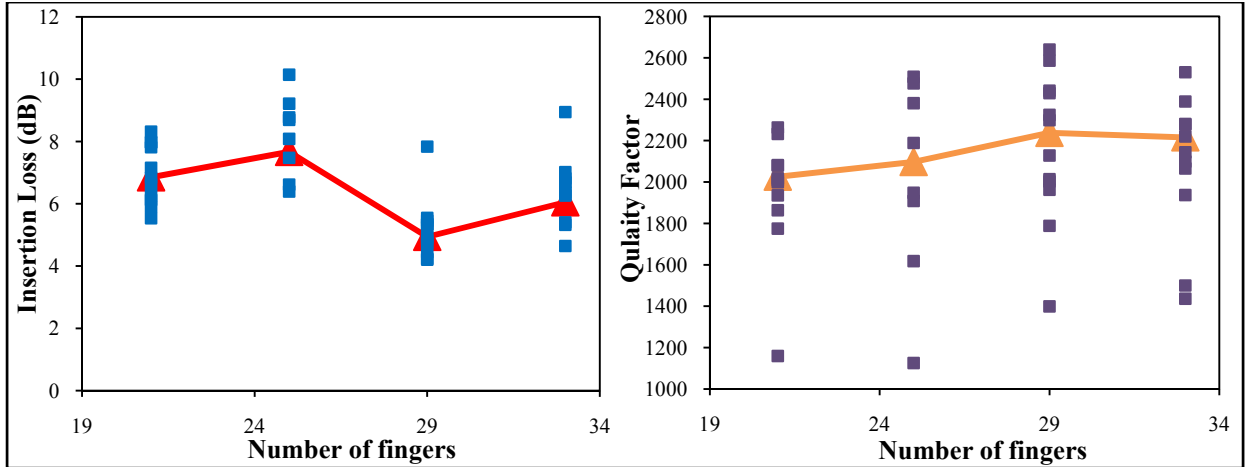
Figure 20- Effect of number of fingers on the insertion loss and the quality factor of a 133.2 µm

long TPoD resonator.

5.3 BEST RESULTS

In this work the goal was to optimize the TPoD resonator to have less than 4dB insertion loss while terminated with standard 50Ω impedances. So, the lateral dimensions of the resonators had to be increased beyond the values that could be simulated using the FEM model in a reasonable time.

Following the discussion in section 5.2, a 29th order harmonic resonator was designed to have a resonance peak at 900MHz. This 205.2 µm ($57 * \lambda/4$) long TPoD resonator has a finger pitch of 7.2µm and is supported by thirteen tethers as depicted in the SEM of Figure 21. The frequency response of this resonator fabricated on the UNCD wafer with Young's modulus of 650 GPa is plotted in Figure 22. The motional impedance of the resonator was calculated by modeling the resonator using Multisim and finding the equivalent electrical circuit (Figure 22). Such low motional impedance (22 Ω) was obtained when the resonator is terminated with the internal 50Ω

impedance of the network analyzer. This resonator was also fabricated on UNCD substrates with Young's modulus of 491 GPa and 933 GPa. Corresponding transmission plots are drawn in Figure 23.

Figure 21- SEM of a ~205μm, 29th order TPoD resonator with thirteen pairs of support tethers.
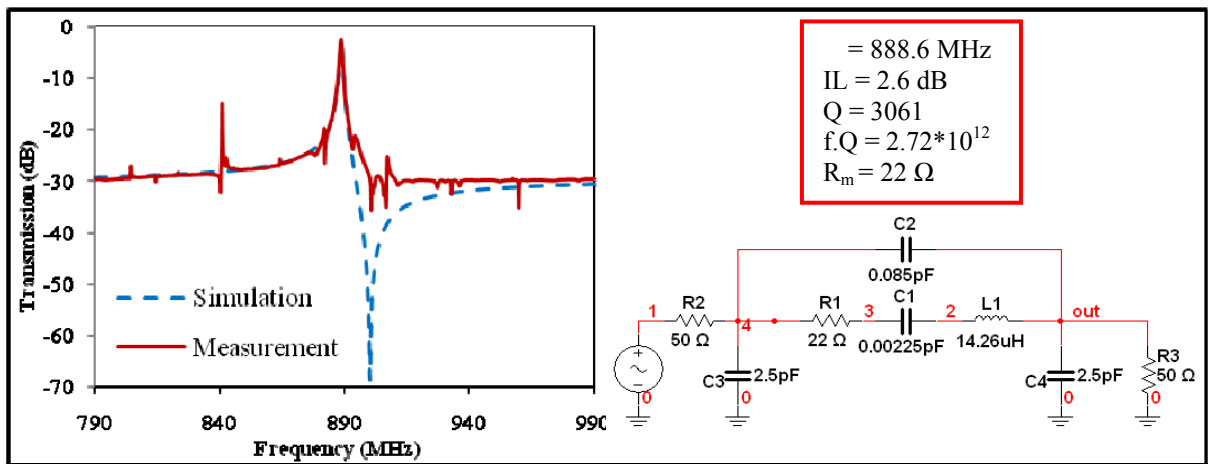
Figure 22- frequency response of the 205 μm long, 29th order harmonic TPoD resonator and the

equivalent electrical circuit.

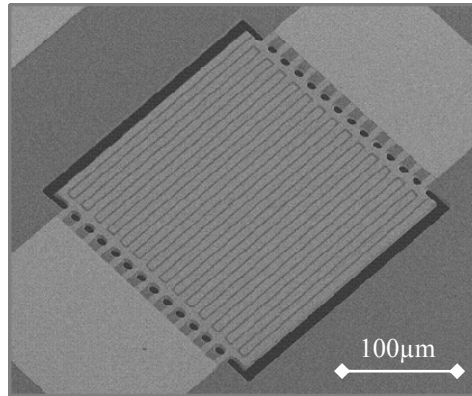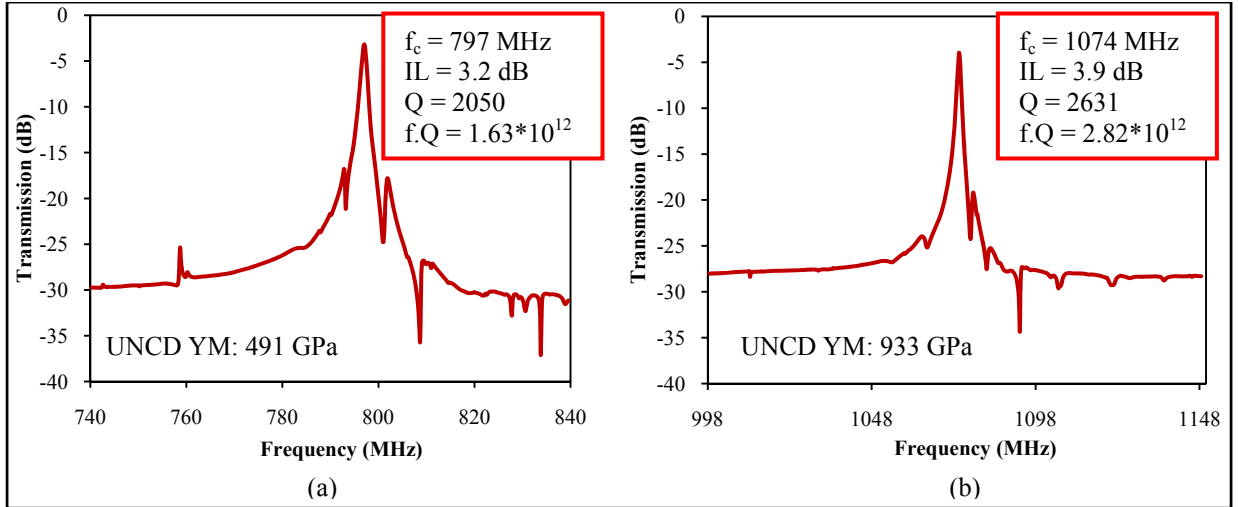Figure 23- Transmission responses of the low-loss 29th order harmonic resonator fabricated on UNCD substrates with Young's modulus of (a) 491GPa and (b) 933GPa.

Also, the temperature coefficient of frequency (TCF) of the TPoD resonator was measured for this low-IL design fabricated on the diamond substrate with 650GPa Young's modulus, and the resonance frequency versus temperature is plotted in Figure 23. TPoS devices fabricated on UNCD substrate show much lower TCF compared to devices fabricated on silicon for which the TCF is in the range from-20 to -30 ppm/°C [19, 12].

To evaluate the power handling of the TPoD resonator, an RF amplifier was used to enable reaching input powers above the limit achievable by the network analyzer (+15 dBm). So, prior to measurements another SOLT calibration was carried out in order to calibrate the measurement setup including the RF amplifier. The frequency response of the resonator at different power levels is plotted in Figure 25. No considerable change is observed in the frequency response of the resonator up to input powers of ~+22 dBm. Above 27 dBm, device broke before going to the bifurcation. At +22 dBm applied power, ~48 mW RMS power was delivered to the device.

Figure 24- Frequency vs. temperature for the 29th order harmonic TPoD resonator fabricated on UNCD substrate with Young's modulus of 650 GPa showing smaller values compared to devices fabricated on silicon.

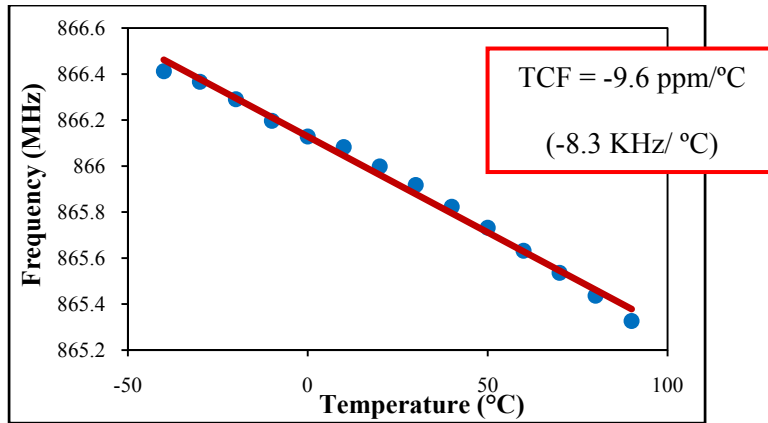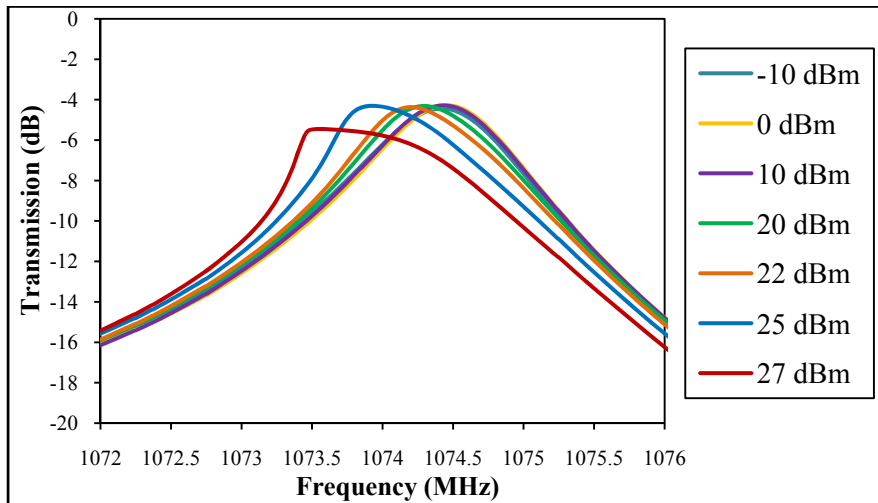Figure 25- Nonlinearity plot of the 29th order TPoD resonator fabricated on UNCD substrate with 650 GPa Young's modulus.

CHAPTER 6

CONCLUSION

This last chapter is a brief conclusion of the work presented in this thesis and also a short summary of the accomplishments. The last section is a short discussion about the future research.

6.1 ACCOMPLISHMENTS

This thesis focused on design and fabrication of thin-film piezoelectric-on-diamond resonators with high quality factor and low motional impedance which can be utilized in filter and oscillator applications. In this thesis, ultrananocrystalline diamond (UNCD) is used as the substrate for fabricating lateral-extensional piezoelectric-on-substrate resonators in order to extend the resonance frequency beyond the limits achievable by silicon. The UNCD films were deposited using hot filament chemical vapor deposition method followed by two polishing steps in order to reduce the surface roughness to promote the growth of high quality piezoelectric thin films, in this case AluminumNitride. Three different UNCD films with different Young's modulus were used to reach frequencies up to two times that of devices fabricated on silicon with the same geometries. The devices fabricated on all of the three UNCD substrates, have different resonance frequencies (from ~500MHz to 1100MHz) and all show improvement compared to the device fabricated on silicon. A FEM model is employed to evaluate the effect of lateral dimensions and support configuration on the performance of the thin-film piezoelectric-on-substrate (TPoS)

resonators in order to achieve very low insertion loss values with standard 50Ω termination impedance. The multi-tethered designs with lengths equal to odd multiples of half-wavelength and support length of $(2n + 1)\,{}^{\lambda}\!/_{4}$ exhibit an improved performance.

Different resonators were designed having various lateral dimensions with different number of support tethers to evaluate the accuracy of the FEM model and to optimize the performance. Finally, a thin-film piezoelectric-on-diamond (TPoD) resonator is reported with a record low insertion loss of 2.6 dB at 888 MHz and $f.Q$ product of $2.72*10^{12}$ while maintaining a very small footprint (205μm x 209μm). The TCF of the TPoD resonator is measured to be -9.6 ppm/°C which is much lower than the devices fabricated on silicon. Also, this TPoD device can withstand input powers up to +22dBm, again higher than the devices fabricated on silicon.

6.2 FUTURE RESEARCH

Lateral-extensional piezoelectric resonators have proved to offer some benefits over other microelectromechanical resonator technologies. These advantages are the better linearity, better power handling capability, and smaller motional impedance. With such low insertion loss, relatively high Q value and since there is no bias voltage required to excite the TPoS resonators, the presented TPoD resonator is a very promising solution to be implemented in an oscillator circuit with low power consumption. However, the support length of the TPoD resonator reported in this work has room for further investigation. The insertion loss of the TPoD resonator can be further reduced for support lengths equal to $\frac{\lambda}{4}$. Also, as reported in [16], by taking advantage of acoustic reflectors, the performance of the TPoS resonator can be further improved. Therefore, it is believed that the IL values can be reduced to values near zero for this class of lateral-extensional piezoelectric resonators. Also, the relatively high power handling capability of the

TPoD resonators requires further study to better understand the limitations and to figure ways to enhance it to a great extent.

On the other hand, there is a high demand for small size, low-loss and narrow-band filters that are suitable for standard 50Ω electronics. Since the resonance frequency of the TPoS resonator can be simply tailored by the structure geometry, these resonators can be designed into a ladder filter configuration. Also, another approach is to couple different resonance modes in order to build higher order filters [20, 21]. The future research will be focusing on designing different classes of high frequency filters with an adjustable fractional bandwidth between 0.1 to few percent.

REFERENCES

[1] C. T.-C Nguyen; "MEMS technology for timing and frequency control," IEEE Transactions on Ultrasonics, Ferroelectrics and Frequency Control, vol.54, no.2, pp.251-270, Feb. 2007.

[2] J. Wang, Z. Ren, and C. T.-C. Nguyen, "1.156-GHz self-aligned vibrating micromechanical disk resonator," IEEE Transactions on Ultrasonics, Ferroelectrics, and Frequency Control, vol. 51, no. 12, pp. 1607-1628, Dec. 2004.

[3] J. R. Clark, H. Wan-Thai, and C. T.-C. Nguyen; "High-Q VHF micromechanical contour-mode disk resonators," Technical Digest of Electron Devices Meeting (IEDM), pp.493-496, Dec. 2000.

[4] L. Yu-Wei, L. Sheng-Shian, X. Yuan, R. Zeying, and C. T.-C Nguyen; "Vibrating micromechanical resonators with solid dielectric capacitive transducer gaps, "Proceedings of IEEE International Frequency Control Symposium, pp. 128-134, Aug. 2005.

[5] S. Pourkamali, A. Hashimura, R. Abdolvand, G. K. Ho, A. Erbil, and F. Ayazi, "High-Q single-crystal silicon HARPSS capacitive beam resonators with self-aligned sub-100-nm transduction gaps," J. Microelectromech. Syst., vol. 12, no. 4, pp. 487–496, Aug. 2003.

[6] Y. Wang, C. Feng, T. Lamers, D. Feld, P. Bradley, and R. Ruby; "FBAR resonator figure of merit improvements," Ultrasonics Symposium (IUS), 2010 IEEE , vol., no., pp.861-863, 11-14 Oct. 2010.

[7] R. Ruby, P. Bradley, Y. Oshmyansky, A. Chien, J. D. Larson; "Thin film bulk wave acoustic resonators (FBAR) for wireless applications," Ultrasonics Symposium, IEEE , vol.1, pp.813-821, 2001.

[8] R. Abdolvand, H. Lavasani, G. Ho, F. Ayazi; "Thin-film piezoelectric-on-silicon resonators for high-frequency reference oscillator applications," IEEE Transactions on Ultrasonics, Ferroelectrics and Frequency Control, vol.55, no.12, pp.2596-2606, Dec. 2008.

[9] B.P. Harrington, M. Shahmohammadi, and R. Abdolvand; "Toward ultimate performance in GHZ MEMS resonators: Low impedance and high Q," IEEE International Conference on Micro Electro Mechanical Systems (MEMS), pp.707-710, Jan. 2010.

[10] G. Piazza, P. J. Stephanou, J. P. Black, R. M. White, and A. P. Pisano; "Single-chip multiple-frequency RF microresonators based on aluminum nitride contour-mode and FBAR technologies," IEEE Ultrasonics Symposium, vol.2, pp. 1187- 1190, Sep. 2005.

[11] M. Rinaldi, C. Zuniga, Z. Chengjie, G. Piazza; "AlN contour-mode resonators for narrow-band filters above 3 GHz," IEEE International Frequency Control Symposium Joint with the 22nd European Frequency and Time forum, pp.70-74, Apr. 2009.

[12] M. Shahmohammadi, B.P. Harrington, and R. Abdolvand, "Concurrent enhancement of Q and power handling in multi-tether high-order extensional resonators," IEEE International Microwave Symposium, pp. 1452-1455, May 2010.

[13] W. Jing, J. E. Butler, D.S.Y. Hsu, and T.-C. Nguyen; "CVD polycrystalline diamond high-Q micromechanical resonators," IEEE International Conference on Micro Electro Mechanical Systems, pp.657-660, 2002.

[14] R. Abdolvand, G. K. Ho, J. Butler, and F. Ayazi, "ZnO-on-nanocrystalline diamond lateral bulk acoustic resonators," IEEE International Conference on Micro Electro Mechanical Systems (MEMS), pp.795-798, Jan. 2007.

[15] H. Fatemi; R. Abdolvand; H. Zeng; J. Carlisle; "Very low-loss high frequency lateral-mode resonators on polished ultrananocrystalline diamond," IEEE International Frequency Control and the European Frequency and Time Forum, pp.1-5, May 2011.

[16] B. P. Harrington and R. Abdolvand, "In-plane acoustic reflectors for reducing effective anchor loss in lateral-extensional MEMS resonators," Journal of Micromech. Microeng. 21, 2011.

[17] O. Auciello, S. Pacheco, A. V. Sumant, C. Gudeman, S. Sampath, A. Datta, R. W. Carpick, V. P. Adiga, P. Zurcher, M. Zhenqiang, H. Yuan; J. Carlisle, B. Kabius, J. Hiller, and S. Srinivasan, "Are Diamonds a MEMS' Best Friend?," Microwave Magazine, IEEE , vol.8, no.6, pp.61-75, Dec. 2007.

[18] R. Abdolvand, Zhili Hao, and F. Ayazi, "A Temperature-Compensated ZnO-on-Diamond Resonant Mass Sensor," IEEE Conference on Sensors, pp. 1297-1300, Oct. 2006.

[19] G. Piazza, P. J. Stephanou, and A. P. Pisano, "Piezoelectric Aluminum Nitride Vibrating Contour-Mode MEMS Resonators," Journal of Microelectromechanical Systems, vol.15, no.6, pp.1406-1418, Dec. 2006.

[20] R. Abdolvand, F. Ayazi, "High-frequency monolithic thin-film piezoelectric-on-substrate filters," J. of Microwave and Wireless Technologies, vol. 1, pp 29-35, 2009.

[21] H. Fatemi, B. P. Harrington, H. Zeng, J. Carlisle, and R. Abdolvand, "50Ω-terminated 900MHz monolithic lateral-extensional piezoelectric filters on ultrananocryslalline diamond," Micro Electro Mechanical Systems (MEMS), 2011 IEEE 24th International Conference on, pp.744-747, Jan. 2011.

VITA

Hediyeh Fatemi

Candidate for the Degree of

Master of Science

Thesis: LOW-IMPEDANCE THIN-FILM AlN-ON-DIAMOND LATERAL-EXTENSIONAL RESONATORS

Major Field: Electrical Engineering

Minor Field: Microelectromechanical Systems

Biographical:

Education:

Completed the requirements for the Master of Science in electrical engineering major at Oklahoma State University, Stillwater, Oklahoma in December, 2011.

Completed the requirements for the Bachelor of Science in electrical engineering at University of Tehran, Tehran, Iran in 2009.

Professional Memberships: IEEE student member since 2007

Name: Hediyeh Fatemi   Date of Degree: December, 2011

Institution: Oklahoma State University   Location: Stillwater, Oklahoma

Title of Study: LOW-IMPEDANCE THIN-FILM AlN-ON-DIAMOND LATERAL-
                EXTENSIONAL RESONATORS

Pages in Study: 40   Candidate for the Degree of Master of Science

Major Field: Electrical Engineering

Minor Field: Microelectromechanical Systems

Scope and Method of Study: The focus of this thesis is the design and fabrication of thin-
    film piezoelectric-on-diamond resonators to have very low insertion loss values.
    Ultrananocrystalline films with different Young's modulus were used as the
    substrate for these resonators in order to extend the resonance frequency beyond
    the limits achievable with silicon. This work is dedicated to investigate different
    techniques to improve the resonator performance. Effect of the lateral geometries
    as well as the support configurations on the insertion loss and the quality factor of
    the resonator were studied.

Findings and Conclusions: The multi-tethered designs with lengths equal to odd multiples
    of half-wavelength and support length of $(2n + 1)^{\lambda}/_{4}$ exhibit an improved
    performance. A thin-film piezoelectric-on-diamond resonator is reported with a
    record low insertion loss of 2.6 dB at 888 MHz and $f.Q$ product of $2.72*10^{12}$
    while maintaining a very small footprint (205μm x 209μm). The TCF of this
    resonator is measured to be -9.6 ppm/ºC which is much lower than the devices
    fabricated on silicon. Also, this TPoD device can withstand input powers up to
    +22dBm, which is higher than the devices fabricated on silicon reported till the
    date.

ADVISER'S APPROVAL: Dr. Reza Abdolvand